Nano Energy 25 (2016) 18–25

Contents lists available at ScienceDirect

Nano Energy

journal homepage: www.elsevier.com/locate/nanoen

Integrated multi-unit transparent triboelectric nanogenerator harvesting rain power for driving electronics

Qijie Liang [a], Xiaoqin Yan [a], Xinqin Liao [a], Yue Zhang [a,b,*]

[a] State Key Laboratory for Advanced Metals and Materials, School of Materials Science and Engineering, University of science and technology Beijing, Beijing 100083, China

[b] The Beijing Municipal Key Laboratory of New Energy Materials and Technologies, University of Science and Technology Beijing, Beijing 100083, China

ARTICLE INFO

Article history:
Received 23 March 2016
Received in revised form
18 April 2016
Accepted 19 April 2016
Available online 20 April 2016

Keywords:
Transparent
Multi-unit triboelectric nanogenerator
Rain power
Driving electronics
Smart systems

ABSTRACT

Transparent and high efficient power sources harvesting energy from ambient environment is a desirable solution to on-site energy demand for organic electronic and optoelectronic devices. Here we report an integrated multi-unit transparent triboelectric nanogenerator (MT-TENG) for harvesting clean energy from ambient water motions. The instantaneous output power density reaches 27.86 mW/m^2, which is 11.6 times of that generated from individual T-TENG with the same working dimension. The output of the MT-TENG can be further enhanced by miniaturizing the size of each single unit. In addition, the rational design of the MT-TENG increases the safety for future practical applications. The influence of temperature and pH value of water on the electric outputs is also systematically studied in consideration of different application environment. Given the compelling features, such as, high efficiency, cost-effective, easily implemented, it has great potential of integrating with building, vehicle or silicon-based solar cell to harvest clean energy from raindrop for powering electronics and constructing smart systems.

1. Introduction

Searching for clean and renewable energy is mandatory for the sustainable development of modern society faced with the challenges of energy crisis and environmental pollution. Harvesting energy form ambient environment has attracted increasing interests for meeting large-scale energy demands and building self-powered sensor systems [1–4]. In the last decade, various types of sensors related to health monitoring, environmental protection, medical care as well as security had been developed and reached every corner of our daily life. Downscaling of energy consumption from each sensor unit and upscaling of the number of units are the two major trends. So harvesting energy from the environment can provide self-powered sensors the advantage of long-term operation and reduce the use of battery materials that cause pollution to the environment. Wind, solar irradiance and water, available in enormous quantities, are renewable and green energy sources with great potential. Among these energy sources, water presenting in the form of raindrop, river flow and ocean tides is a promising candidate, because it contains inexhaustible energy and has little dependence on daytime, season and weather.

The general approach for harvesting energy from water motion is electromagnetic generator [5–8]. In principle, the turbine of the power plant is driven to rotate by water falling through a vertical distance. Mechanical kinetic energy form water is transformed into electricity with the electromagnetic generator of the hydroelectric power plant based on electromagnetic effect.

Hydroelectric power has been one of the major forms of energy supply. But such power plant is designed for large-scale blue energy harvesting. Not all of the forms of water motions are suitable for driving the turbine of the power plant, because the electromagnetic generator is bulky and heavy due to the presence of magnets and metal coils. For example, the energy from water in our residential area, such as washroom, home faucet as well as in agricultural irrigation and industry cannot be effectively harvested.

As mentioned above, small-scale energy harvesting is also a topic with growing interest. Harvesting energy from ambient environment has the feasibility of powering sensor system or electronic instruments owing to the downscaling of energy consumption of sensor or other electronics. In 2012, a new type of generator based on contact electrification and electrostatic induction was invented. The triboelectric nanogenerator (TENG) [9–19] has been demonstrated to be a light weight, cost-effective and reliable device to effectively collect clean energy from environmental sources. When two dissimilar materials differed in polarity of triboelectricity are periodically contacted and separated, the

* Corresponding author at: State Key Laboratory for Advanced Metals and Materials, School of Materials Science and Engineering, University of science and technology Beijing, Beijing 100083, China.
E-mail addresses: xqyan@mater.ustb.edu.cn (X. Yan), yuezhang@ustb.edu.cn (Y. Zhang).

http://dx.doi.org/10.1016/j.nanoen.2016.04.033
2211-2855/

potential difference between two electrodes varies, which drives electrons to transfer through an external load and continuous outputs are generated [20–22]. Recently, by applying the triboelectrification between water and solid/air interfaces, a water-based triboelectric nanogenerator [23–28] has been developed for harvesting energy from water flow. On the other hand, transparent and high efficient power source is an important component of optoelectronic and organic electronic devices. The transparent characteristic is also a required feature in the design of many functional devices. In practical applications, triboelectric nanogenerator should be highly transparent to be integrated with building, vehicle glass or even with silicon-based solar cell for harvesting energy from raindrop. In addition, several requirements should be concerned including: simple structure, high efficiency, low cost, strong adhesion, stable and safe service.

With regards to these concerns, we designed a integrated multi-unit transparent triboelectric nanogenerator (MT-TENG) for green energy harvesting. The efficiency of the MT-TENG has been greatly improved comparing with that of the individual T-TENG with the same working dimension. And it can be further enhanced by miniaturizing the size of each unit in the MT-TENG. As a type of energy device, the output power density of the integrated multi-unit transparent triboelectric nanogenerator (MT-TENG) reaches 27.86 mW/m^2, which is 2.5 times of the state-of-the-art output of individual T-TENG [11] of 11.56 mW/m^2. Besides, the rational design of the MT-TENG is capable of overcoming the complete failure problem facing the water-based T-TENG. The maximum transmittance of the MT-TENG is 84.57% with the organic film as anti-reflection coating. The dependence of temperature and pH value of water on the electric outputs is also systematically studied in consideration of different application environment. Given the simple structure, high efficiency, low cost, stable and safe service, the MT-TENG renders a promising way towards green energy harvesting for powering electronics and constructing smart systems.

2. Methods

2.1. Fabrication of a MT-TENG

The fabrication process started with cutting the FTO glass substrate into a rectangular (30 mm*50 mm). Than the glass substrate was ultrasonically cleaned in acetone, isopropyl alcohol for 10 min. The kapton film was adhered onto the FTO glass as a mask for following wet chemical etching procedure and the gap distance between two strips was 2 mm. The etching process was carried out with hydrochloric acid (0.5 M) and zinc powder. To prevent electric leakage, the edge of FTO glass substrate was also eliminated like previous method. Subsequently, the FTO glass was spin-coated with non-purified PTFE suspension at 1000 rpm for 10 s after being cleaned by ethanol and water. The thickness of PTFE film can be adjusted by diluting the suspension proportionally. The film-covered substrate was heated at 380 °C for 10 min. Finally, copper wires were connected to the FTO electrodes for subsequent electrical measurements. The working area of all kinds of MT-TENG was 28 mm*32 mm.

2.2. Characterization

The morphology and thickness of the prepared PTFE film were investigated by field emission scanning electron microscopy (FEI Quanta 3D). Atomic Force Microscopy (Multi-mode 3, Bruker) was used to study the surface morphology of the PTFE film. The transmittances of the fabricated MT-TENG were characterized by the UV–vis spectroscopy (Agilent Cary 5000 spectrophotometer). The flowing water form household faucet was applied to the MT-TENG for electrical measurements. A digital oscilloscope (RIGOL, DS4052) and a low noise current preamplifier (Stanford SR570) were used to test the electric outputs of the MT-TENG. The entire measurements were carried out in ambient environment.

3. Results and discussions

The fabricated MT-TENG is a fully integrated device constituted by a glass substrate, fluorine-doped tin oxide (FTO) electrode array and PTFE film. PTFE film is chosen due to its attractive properties including good chemical, thermal stability, low friction coefficient and excellent mechanical strength. In addition, The developed MT-TENG is capable of working under harsh environment and has resistance to acid, alkali and high temperature due to the high chemical, thermal stability and good mechanical strength for PTFE film. The schematic diagram is illustrated in Fig. 1(a). Parallel strip-shaped FTO electrodes serve as the electrode of each unit in the NT-HENG. Fig. 1(b) shows the fabrication process of the MT-TENG.

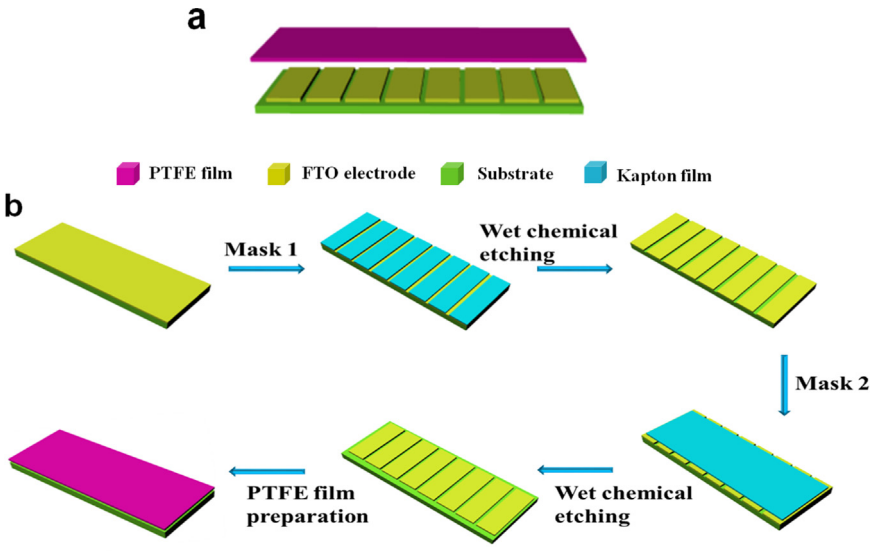

Fig. 1. Schematic diagram (a) and fabrication process (b) of the MT-TENG.

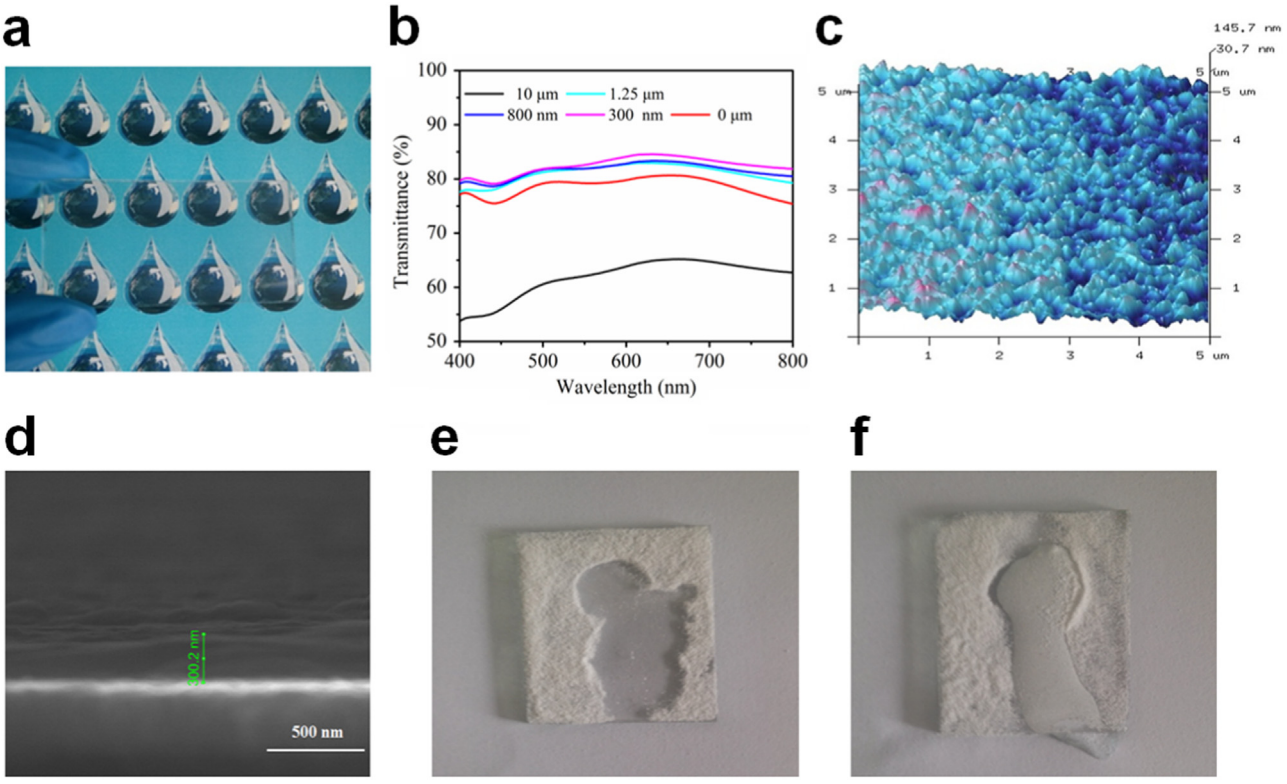

Fig. 2. (a) Photograph showing the high transmittance of the fabricated MT-TENG. (b) The UV–vis spectra of the as-prepared devices with different thicknesses of PTFE film. (c) The AFM image of the surface topography of the fabricated PTFE film. (d) Scanning electron microscopy (SEM) image of cross section of the MT-TENG. (e)-(f) With and without self-cleaning characteristic of MT-TENG (e) and ordinary glass (f). The white powder is polystyrene.

The fabrication starts from the design of the FTO electrode array. Kapton film was utilized as the mask and firstly attached to the FTO electrode with a fixed gap. Then the FTO electrode covered by kapton film was etched by a wet chemical etching process. Subsequently, the treated glass was applied with another etching process to eliminate FTO on the edge. This is important for the avoidance of short circuit issue. Specifically, the glass with FTO electrode array was overlaid with another kapton film, followed by a wet chemical etching process. Finally, the prepared substrate was spin-coated with a non-purified and diluted PTFE suspension to form transparent hydrophobic functional film.

Fig. 2(a) shows the photograph of a fabricated MT-TENG on the paper with alphabets, indicating the high transmittance of the MT-TENG. UV–vis spectroscopy was utilized to systematically characterize the transparency of the fabricated MT-TENG with different thickness of PTFE film, as depicted in Fig. 2(b). The maximum transmittance of the T-HENG is 84.57% with the PTFE film thickness of 300 nm. Interestingly, compared with the sole FTO glass substrate, the transmittance of the fabricated MT-TENG with the thickness of PTFE film below 1.25 μm is larger. This imply that the PTFE film play a role of antireflection coating, [29–31] which is used extensively in optical devices to reduce the surface reflection. Two conditions must be fulfilled for an ideal homogeneous antireflection coating [32]:

$$n_1 = \sqrt{n_0 n_1} \tag{1}$$

$$d = \frac{(2k+1)\lambda}{4n_1} \tag{2}$$

Where n_0, n_1, n_2 represent the refractive indices of air, PTFE film and FTO electrode, respectively. λ is the wavelength of the light. So controlling the thickness of the PTFE film is capable of enhancing the transmittance of the MT-TENG with PTFE film acting as an antireflection coating, under condition that the refractive index of the PTFE film is between that of the FTO electrode and air. The other reason for manipulating the thickness of PTFE film is to decrease the light absorbed by film. As illustrated in Fig. 2(b), the transmittance of the MT-TENG will greatly attenuate with the thickness of PTFE film being 10 μm.

The topography of the PTFE film was investigated by atomic force microscope (AFM). The surface morphology is constituted of irregular nanostructures with roughness of 53 nm (Fig. 2(c)). Fig. 2 (d) displays the cross-sectional scanning electron microscopy (SEM) image of the fabricated MT-TENG. The thickness of the prepared PTFE film is 300.2 nm.

PTFE film is a fluoropolymer with very low surface energy that makes it a hydrophobic surface which is of great significance in separating between water-drop and PTFE surface. The fabricated MT-TENG also exhibited a self-cleaning character by applying the hydrophobic PTFE film. In the experiment, polystyrene powder was sprayed to create a dusty surface. As shown in Fig. 2(e), the polystyrene powder was removed with the water dropped on the MT-TENG. By contrast, the powder was not eliminated and merely redistributed by water drop (Fig. 2(f)).

To measure the electric output of the MT-TENG, we applied a household faucet to provide flowing water with settled flow. The flowing rate of water was maintained at 45 ml/s, and the tilt angle was optimized at 10°. The distance between the device and the faucet was fixed at 20 cm. The output voltage of the MT-TENG and individual T-TENG with the same working area was exhibited in Fig. 3(a). The output voltage of each unit in the MT-TENG is the same or larger than that of the individual T-TENG. The maximum output voltage of is 5.3 V. Fig. 3(b) displayed the output current density of the MT-TENG and individual T-TENG. The output current density of every unit in the MT-TENG is 7–10 times of that of the

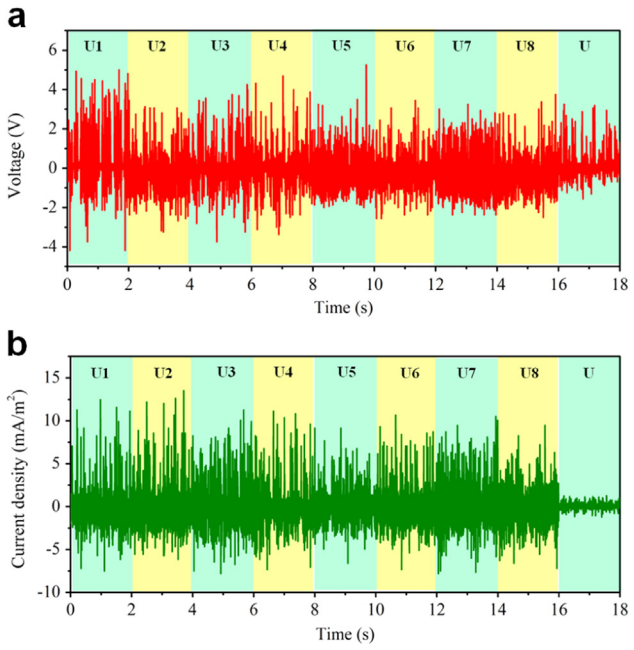

Fig. 3. Results of the electrical measurements. (a) Output voltages and (b) output current densities of MT-TENG and individual T-TENG. U1-U8 are the eight units of the MT-TENG and U represents the individual T-TENG.

individual T-TENG, and the maximum output density of the MT-TENG is 13.1 mA/m^2. Comparing with individual T-TENG, each unit in the MT-TENG delivered a same size of the output voltage and a largely enhanced output current density.

Above experiment results indicated that the rational structure design of the integrated multi-unit transparent triboelectric nanogenerator attributes to the enhanced efficiency for harvesting water energy, comparing with individual transparent triboelectric nanogenerator (T-TENG). The fundamental working principle of the MT-TENG is schematically depicted in Fig. 4. The electricity generation is based on a sequential contact electrification and electrostatic induction process. Both the MT-TENG and individual T-TENG are operated in single-electrode mode. For simplification, positively charged water drop is chosen to illustrate the energy transformation process. As pointed out by some previous studies, water falling through air or travelling through an insulating tube will contain triboelectric charges on its surface due to the friction with tube or air (Stage 1). When the charged water drop approaches the PTFE film, a positive potential difference will be formed between the FTO electrode and ground, driving electrons to be transferred from ground to the FTO electrode (Stage 2). This process produces a positive current pulse and will last until the potential difference is completely balanced (Stage 3). For individual T-TENG, no output will be generated with the maintained equilibrium state disrupted by the departure of the water drop. But for MT-TENG, a negative potential difference will be created between the electrode of the first unit and ground as water drop leaves the first unit. Electrons flow back from the first electrode to ground, producing a negative current pulse (Stage 4). Then water drop continues to slide down and reaches the film above the second electrode, a positive current pulse is obtained just like the aforementioned process (Stage 5). When water drop leaves the PTFE film of the individual T-TENG and MT-TENG, a negative current pulse signal is achieved (Stage 6). With regard to a full energy transformation process, the individual T-HENG generates a cycle of alternating current signal. For the MT-TENG, multiple cycles of current signal corresponding to the amount of units in the MT-TENG can be acquired. So the structure design of the MT-TENG facilitates the shortening of the equilibrium state of individual T-TENG, increasing the transferred charges, thus the efficiency of the MT-TENG is largely enhanced, as compared to individual T-TENG.

Here, three categories of factors were investigated to study how to regulate the electric output of the MT-TENG, i.e., the amount of units of the MT-TENG, water temperature, and pH value of the water.

First, design parameters, especially the amount of units in the MT-TENG have a decisive effect on the electric output of the T-TENG. The major goal of the design of MT-TENG is to improve the efficiency for harvesting water energy. The rational design of the MT-TENG is capable of facilitating the transfer of charges, and thus

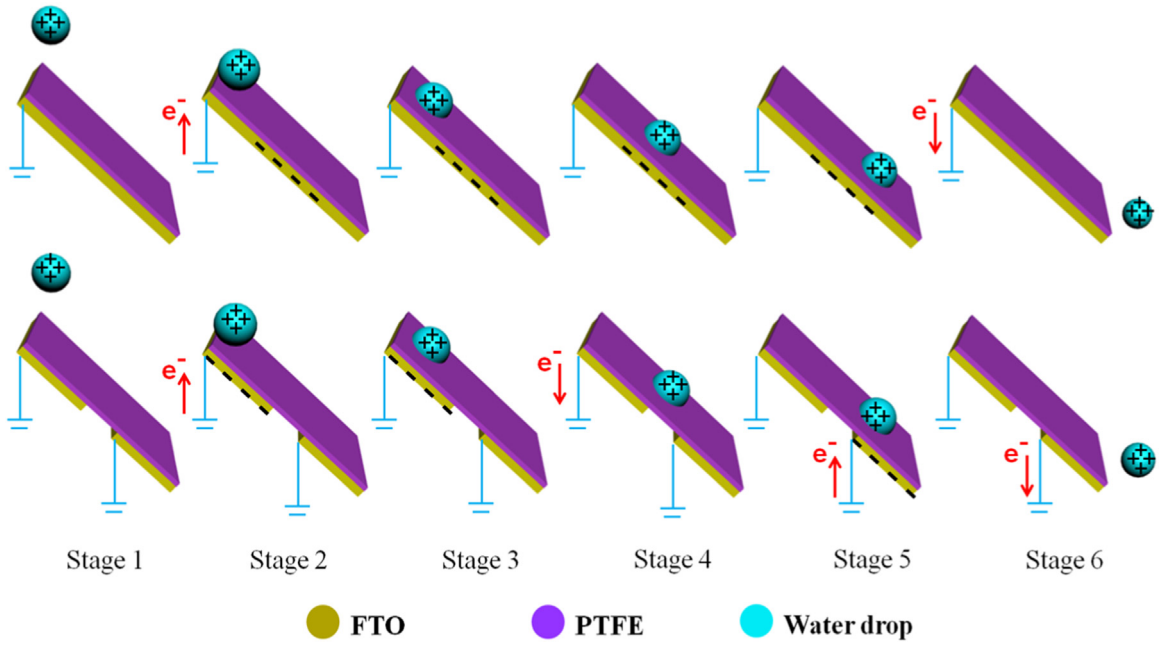

Fig. 4. Working mechanism illustration of the improved efficiency of the MT-TENG comparing with individual T-TENG.

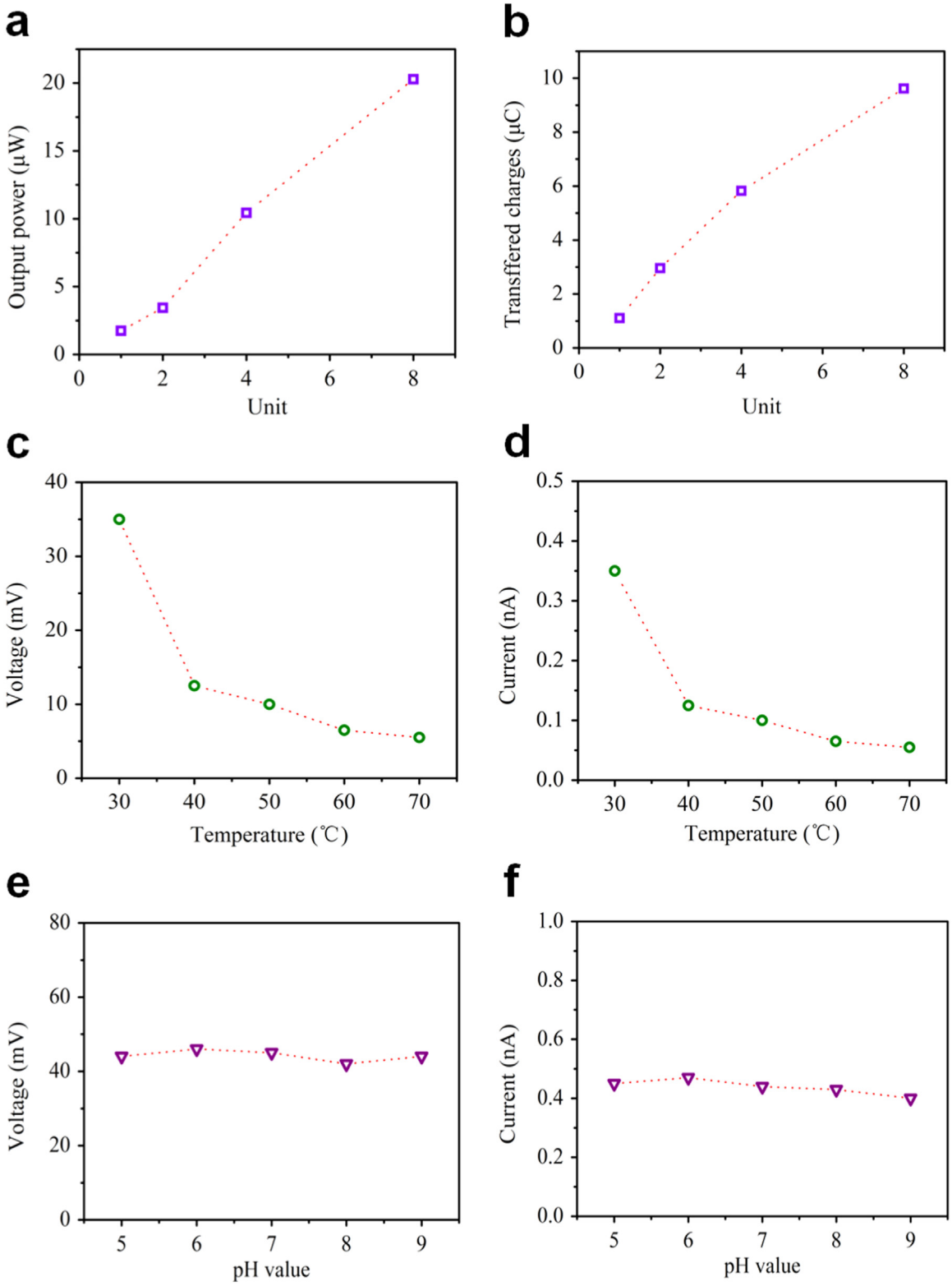

Fig. 5. Investigation on factors that influence the electric output. (a) Output power with increasing units. (b) Transferred charges with increasing units. (c) Output voltage with increasing temperature of water. (d) Output current with increasing temperature of water. (e) Output voltage with pH value of water. (f) Output current with pH value of water.

enhancing the efficiency of the T-TENG. As revealed in Fig. 5(a), the output power increases from 1.75 μW to 20.3 μW with the amount of units varying from 1 to 8. The transferred charges increase with the increase of the amount of units in the MT-TENG, as shown in Fig. 5(b). Theoretically, the transferred charges in the external load of T-TENG can be expressed as [14]:

$$Q = -\frac{Q_w d_1}{d_2 \varepsilon_{rp} + d_1} \tag{3}$$

Where Q_w is the charges on the water drop surface, d_1 and d_2 are

the thickness of the fabricated transparent PTFE film and the distance between water drop and PTFE film, respectively. ε_{rp} is the relative permittivity of PTFE film. Given that the charges on the water drop surfaces keep constant during the process of contact-separation between water drop and PTFE film. For an individual T-TENG, the transferred charges Q_I in one cycle are:

$$Q_I = 2Q_w \tag{4}$$

For MT-TENG with n units, the transferred charges Q_N in one cycle are:

$$Q_n = 2nQ_w \tag{5}$$

So the MT-TENG facilitates the process of charge transfer, comparing with individual T-TENG. This design of MT-TENG is on the basis of that the output power follows no linear relationship with the working area of T-TENG. As studied in previous work, [33] for this single-electrode TENG, it will generate no output when the working dimension becomes infinite, because the fully electrostatic shield condition. Above experimental results verifies that the design of MT-TENG improves the efficiency for harvesting water energy.

Second, temperature is a major factor that influences the electric output. As displayed in Fig. 5(c), both the output current and voltage decrease with the temperature varying from 30° to 70°. Temperature has been regarded as a key factor to affect the dielectric constant and polarity of water [34]:

$$-10^6\left(\frac{\partial^2 lnD}{\partial^2 lnD}\right) = 2a_1 + 4a_2t + 4a_3p + 8a_4pt \tag{6}$$

Where D is the dielectric constant of water, P, a_1, a_2, a_3, a_4 are constant, and t is temperature of water. The increase of temperature can lead to the decrease of dielectric constant and increase of conductivity. Consequently, the triboelectric charge density reduces and results in the decrease of the output of the MT-TENG. Above result indicate that the MT-TENG can be applied to be a temperature sensor of water or to detect substances that change the dielectric and polarity of water.

Third, for different applications, water with pH value of 4–9 can be applied to the MT-TENG. For example, the typical pH value of raindrop varies from 5.6 to 7.5. So the influence of pH value on the electric output of the MT-TENG was investigated. As revealed in Fig. 5(e), (f), the output voltage and current did not show an obvious variation with pH value increasing from 5 to 9, which means that the MT-TENG can maintain its high performance when applied in different applications. This is of great significance in expanding the application area of the MT-TENG.

For different applications, the MT-TENG will be connected to external loads with variable resistance. The output changes with the variation of load resistance. In view of this point, resistors were connected to a unit in the MT-TENG to systematically investigate the dependence of the output performance on different external loads. The flowing rate was settled to be 45 ml/s. As illustrated in Fig. 6(a), the output voltage increases from 0.18 V to 2.86 V with the load raised from 0.1 MΩ to 10 MΩ. The output current follows a reversed tendency that it decreased from 1.8 μA to 70 nA under the same external load (Fig. 6(b)). Consequently, the instantaneous power density on the load remains small below 0.1 MΩ, and reaches the maximum value of 12.66 mW/m^2 at a resistance of 0.5 MΩ (Fig. 6(c)). The measurement results revealed that the MT-TENG achieves its highest efficiency for harvesting water energy with the external load on the order of a fraction of megaohm.

For future applications, integrating more units and ensuring the safe service are essential. As mentioned above, the entire preparation process is straightforward and low cost, demonstrating that this approach can be utilized to prepare large-scale T-TENG which is of great significance for the MT-TENG to achieve practical applications. Fig. 7(a) exhibited the photograph of an as-prepared MT-TENG with dimension of 150 mm × 200 mm, which demonstrated the feasibility of fabrication on large scale for practical application. The schematic diagram of MT-TENG with hundreds of units was displayed in Fig. 7(b). On the other hand, the design of the MT-TENG enhanced the safety for its future service. Because each unit in the device performs independently, the invalidation of a couple of units will not have an effect on the normal operation of the remaining units (Fig. 7(d)). But for individual T-TENG, imperfect encapsulation or incidental damage will cause the whole device catastrophic failure (Fig. 7(c)). For the demand of safe and stable running of T-TENG, this is unacceptable for the future practical application. Fig. 7(e)-(f) illustrated the design that the MT-TENG was integrated with vehicle glasses, building glasses for harvesting clean energy from raindrop. The harvested energy can be utilized to drive LCD screen (Inset of Fig. 7(e)) or other electronics, which is utmost importance in powering sensors and constructing smart systems.

Compared with previous multi-layer TENG [35], the two kinds of TENG have different working mechanisms, the multi-layer TENG is based on free-standing mode and our MT-TENG is on single-electrode mode. The electricity generation process of the multi-layer TENG is generated with the movement of a moving part triggering by movement, while our MT-TENG is with the contact and separation processes between water drop and the functional film of the device. Besides, our MT-TENG is a transparent triboelectric nanogenerator while the listed work is not. Last but not least, our device is a glass-based transparent device that can be used to harvesting energy from rain.

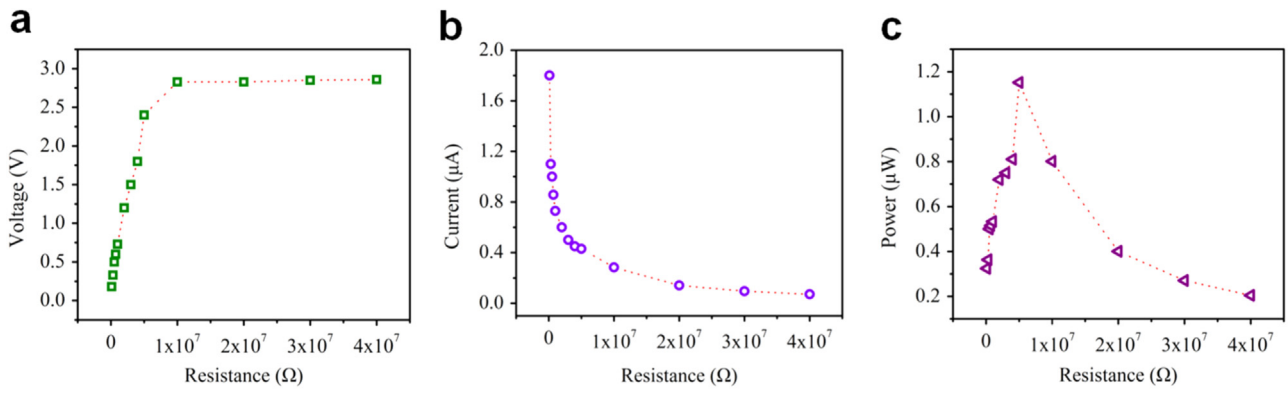

Fig. 6. Results of load matching test of the MT-TENG. (a) Amplitude of voltage with increasing load resistance. (b) Current with increasing load resistance. (c) Output power with increasing load resistance.

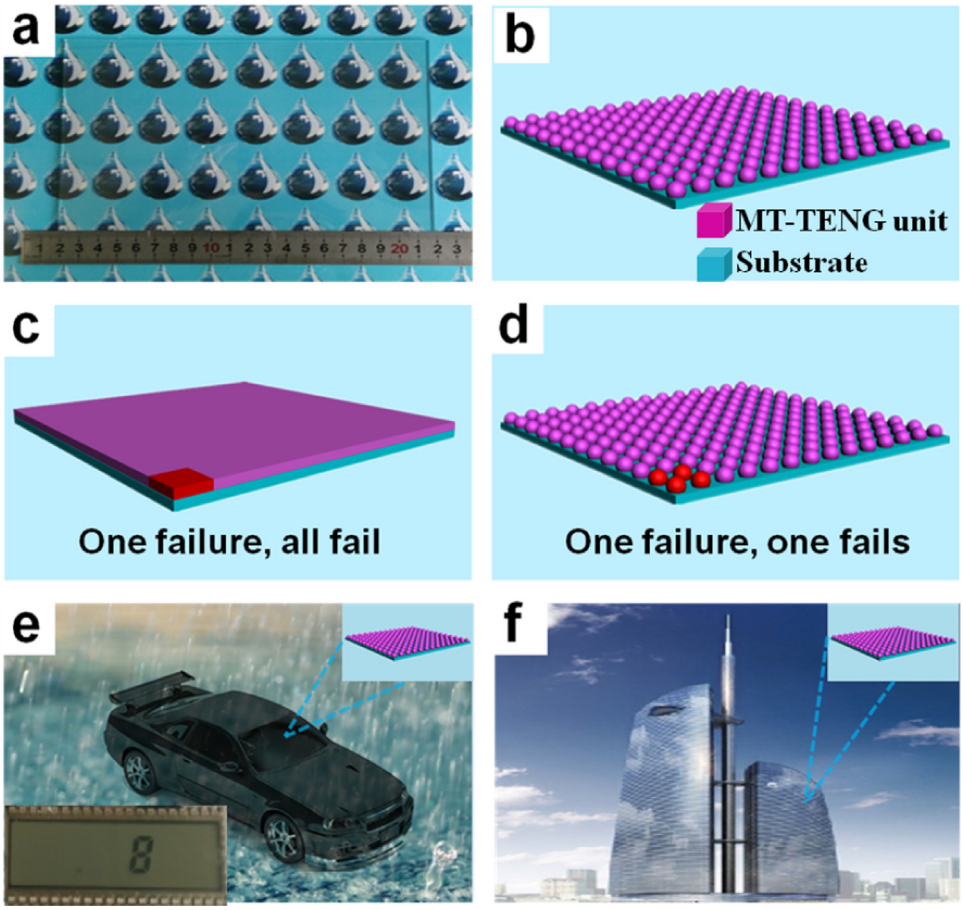

Fig. 7. (a) Photograph showing that the MT-TENG (15 cm*20 cm) can be fabricated on large area. (b) Schematic illustration of the MT-TENG with hundreds of units. (c)-(d) The comparing of service behavior between MT-TENG and individual T-TENG. Red zone represents the damaged parts. (e)-(f) Demonstration on the potential applications of the MT-TENG in integrating with vehicle and building. Inset is the lightened LCD screen with the harvested energy.

4. Conclusions

In summary, an integrated multi-unit transparent triboelectric nanogenerator has been developed to harvest water energy in ambient environment for powering electronics. With the introduction of "Top-Down" and "Bottom-Up" methods to its structure design, the MT-TENG can significantly improve the efficiency of the nanogenerator by facilitating charge transfer. At a flowing rate of 45 ml/s, the output power density of the multi-unit is 27.86 mW/m^2, which is 11.6 times as high as that of individual T-TENG with the same working dimension. This can be further enhanced by miniaturizing the size of each single unit or applying superhydrophobic nanostructures as functional materials. In addition, the design of the MT-TENG also ensures the safely and effective service for its future applications. The dependence of the electrical output on the temperature and pH value of water has been systematically studied. In a word, the integrated multi-unit transparent triboelectric nanogenerator has great potential of harvesting clean water-related energy from ambient environment for directly powering electronics and building smart systems.

Acknowledgments

The contributions of Yukang Zhang, Wei Li, Ningyang Shen, Tongtong Lv and Pengyuan Huang on device fabrication and performance investigation are really appreciated. This work was supported by the National Major Research Program of China (2013CB932602), the Major Project of International Cooperation and Exchanges (2012DFA50990), the Program of Introducing Talents of Discipline to Universities (B14003), NSFC (51232001, 51172022, 51372023, 51372020), the Fundamental Research Funds for the Central Universities (FRF-AS-B-001A).

References

[1] R. Byrne, D. Diamond, Nat. Mater. 5 (2006) 421–424.
[2] Y. Zhang, X. Yan, Y. Yang, Y. Huang, Q. Liao, J. Qi, Adv. Mater. 24 (2012) 4647–4655.
[3] Z.-H. Lin, G. Zhu, Y.S. Zhou, Y. Yang, P. Bai, J. Chen, Z.L. Wang, Angew. Chem. Int. Ed. 52 (2013) 5065–5069.
[4] S. Chen, C. Gao, W. Tang, H. Zhu, Y. Han, Q. Jiang, T. Li, X. Cao, Z. Wang, Nano Energy 14 (2015) 217–225.
[5] C.R. Saha, T. O'Donnell, N. Wang, R. McCloskey, Sens. Actuators a-Phys. 147 (2008) 248–253.
[6] S.P. Beeby, R.N. Torah, M.J. Tudor, P. Glynne-Jones, T. O'Donnell, C.R. Saha, S. Roy, J. Micromech. Microeng. 17 (2007) 1257–1265.
[7] S. Kulkarni, S. Roy, T. O'Donnell, S. Beeby, J. Tudor, J. Appl. Phys. (2006), http://dx.doi.org/10.1063/1.2176089.
[8] P. Glynne-Jones, M.J. Tudor, S.P. Beeby, N.M. White, Sens. Actuators a-Phys. 110 (2004) 344–349.
[9] F. Yi, L. Lin, S. Niu, P.K. Yang, Z. Wang, J. Chen, Y. Zhou, Y. Zi, J. Wang, Q. Liao, Y. Zhang, Z.L. Wang, Adv. Funct. Mater. 25 (2015) 3688–3696.
[10] J. Yang, J. Chen, Y. Su, Q. Jing, Z. Li, F. Yi, X. Wen, Z. Wang, Z.L. Wang, Adv. Mater. 27 (2005) 1316–1326.
[11] Q. Liang, X. Yan, Y. Gu, K. Zhang, M. Liang, S. Lu, X. Zheng, Y. Zhang, Sci. Rep. 5 (2015) 9080.
[12] G. Zhu, J. Chen, T. Zhang, Q. Jing, Z.L. Wang, Nat. Commun. 5 (2014) 3426.
[13] Yang, J. Chen, Y. Yang, H. Zhang, W. Yang, P. Bai, Y. Su, Z.L. Wang, Adv. Energy Mater. (2014), http://dx.doi.org/10.1002/aenm.201301322.
[14] Q. Liang, Z. Zhanga, X. Yan, Y. Gu, Y. Zhao, G. Zhang, S. Lu, Q. Liao, Y. Zhang, Nano Energy 14 (2015) 209–216.
[15] F.-R. Fan, Z.-Q. Tian, Z.L. Wang, Nano Energy 1 (2012) 328–334.

[16] Q. Liang, X. Yan, X. Liao, S. Cao, X. Zheng, H. Si, S. Lu, Y. Zhang, Nano Energy 16 (2015) 329–338.
[17] G. Zhu, Y.S. Zhou, P. Bai, X.S. Meng, Q. Jing, J. Chen, Z.L. Wang, Adv. Mater. 26 (2014) 3788–3796.
[18] L. Zheng, Z.-H. Lin, G. Cheng, W. Wu, X. Wen, S. Lee, Z.L. Wang, Nano Energy 9 (2014) 291–300.
[19] Y. Yang, G. Zhu, H. Zhang, J. Chen, X. Zhong, Z.-H. Lin, Y. Su, P. Bai, X. Wen, Z. L. Wang, ACS Nano 7 (2013) 9461–9468.
[20] W. Tang, J. Tian, Q. Zheng, L. Yan, J. Wang, Z. Li, Z.L. Wang, ACS Nano 9 (2015) 7867–7873.
[21] Z. Li, J. Chen, J. Yang, Y. Su, X. Fan, Y. Wu, C. Yu, Z.L. Wang, Energy Environ. Sci. 8 (2015) 887–896.
[22] J. Chen, G. Zhu, J. Yang, Q. Jing, P. Bai, W. Yang, X. Qi, Y. Su, Z.L. Wang, ACS Nano 9 (2015) 105–116.
[23] Y. Su, X. Wen, G. Zhu, J. Yang, J. Chen, P. Bai, Z. Wu, Y. Jiang, Z. Lin Wang, Nano Energy 9 (2014) 186–195.
[24] Z.-H. Lin, G. Cheng, S. Lee, K.C. Pradel, Z.L. Wang, Adv. Mater. 26 (2014) 4690–4696.
[25] Z.-H. Lin, G. Cheng, L. Lin, S. Lee, Z.L. Wang, Angew. Chem. Int. Ed. 52 (2013) 12545–12549.
[26] L. Zheng, G. Cheng, J. Chen, L. Lin, J. Wang, Y. Liu, H. Li, Z.L. Wang, Adv. Energy Mater. 5 (2015) 1501152.
[27] G. Cheng, L. Zheng, Z.-H. Lin, J. Yang, Z. Du, Z.L. Wang, Adv. Energy Mater. 5 (2015) 1401452.
[28] G. Cheng, Z.-H. Lin, Z.-l. Du, Z.L. Wang, ACS Nano 8 (2014) 1932–1939.
[29] H.-T. Chen, J. Zhou, J.F. O'Hara, F. Chen, A.K. Azad, A.J. Taylor, Phys. Rev. Lett. 105 (2010) 073901.
[30] X.-T. Zhang, O. Sato, M. Taguchi, Y. Einaga, T. Murakami, A. Fujishima, Chem. Mater. 17 (2005) 696–700.
[31] S. Walheim, E. Schaffer, J. Mlynek, U. Steiner, Science 283 (1999) 520–522.
[32] W.-L. Min, B. Jiang, P. Jiang, Adv. Mater. 20 (2008) 3914–3918.
[33] Sm Niu, Z.L. Wang, Nano Energy 14 (2015) 161–192.
[34] G.C. Akerlof, H.I. Oshry, J. Am. Chem. Soc. 72 (1950) 2844–2847.
[35] Z.-H. Lin, G. Cheng, X. Li, P.-K. Yang, X. Wen, Z. Lin Wang, Nano Energy 15 (2015) 256–265.

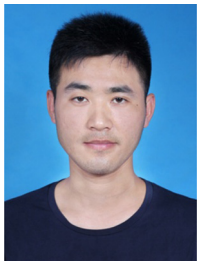

Qijie Liang received his B. S. degree in Materials Science and Engineering from Anhui Jianzhu University in 2012. He is a Ph.D. candidate at physics and chemistry of material, University of Science & Technology Beijing. His research interests include nanogenerators and self-powered systems.

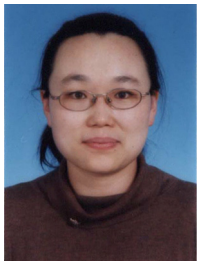

Xiaoqin Yan received her B. S. degree in Materials Science and Engineering from Taiyuan University of Technology in 1997. She got her Ph.D. degree from Institute of Physics, Chinese Academy of Sciences in 2004. She holds a postdoc position at the Institute for Materials Research, Tohoku University. She was promoted to full professor in 2007 at University of Science & Technology Beijing. Her research interests include fabrication and characterization of patterned nanomaterials, design and application of energy conversion and storage devices/system.

Xinqin Liao received his B. S. degree from Fuzhou University in 2012 and now is a Ph.D. student at School of materials science and Engineering in University of Science and Technology Beijing. His research interests include synthesis of nanomaterials for strain sensors, e-skins.

Yue Zhang is a professor of Material Physics of University of Science and Technology Beijing, China. He has been awarded the financial support for outstanding young scientist foundation of China and selected as the chief scientist of Major National Scientific Research Projects. His research focuses on functional nano-materials and nano-devices, new energy materials, and nanoscale failure and service behavior. He has published more than 300 papers in peer reviewed scientific journals and 8 monograph, and held 34 patents in his research area. His publication has been cited more than 5000 times by peers.